electronics

MDPI

Article

Optimal PEM Fuel Cell Model Using a Novel Circle Search Algorithm

Mohammed H. Qais [1], Hany M. Hasanien [2,*], Rania A. Turky [3], Saad Alghuwainem [4], Ka-Hong Loo [5] and Mohmmed Elgendy [6]

[1] Centre for Advances in Reliability and Safety, Hong Kong; mohqais@cairs.hk
[2] Electrical Power and Machines Department, Faculty of Engineering, Ain Shams University, Cairo 11517, Egypt
[3] Electrical Engineering Department, Faculty of Engineering and Technology, Future University in Egypt, Cairo 11835, Egypt; rania.turky@fue.edu.eg
[4] Electrical Engineering Department, College of Engineering, King Saud University, Riyadh 11421, Saudi Arabia; saadalgh@ksu.edu.sa
[5] Department of Electronic and Information Engineering, The Hong Kong Polytechnic University, Hong Kong; kh.loo@polyu.edu.hk
[6] School of Engineering, Newcastle University, Newcastle upon Tyne NE3 4ES, UK; mohammed.elgendy@newcastle.ac.uk
* Correspondence: hanyhasanien@ieee.org

Abstract: The aim of this article is to introduce a novel Circle Search Algorithm (CSA) with the purpose of obtaining a precise electrical model of a proton exchange membrane fuel cell (PEMFC). Current-voltage and current-power curves are used to characterize the performance of PEMFCs. A nonlinear model with seven unknown parameters is used to describe these polarization curves. Estimating these unknown parameters is a critical issue because they influence the dynamic analysis of fuel cells in a variety of applications such as transportation and smart grids. The suggested method is based on minimizing the fitness function (the sum of the squared errors (SSE)) between estimated and measured voltage values. The CSA is compared to the neural network algorithm (NNA), grey wolf optimization (GWO), and the sine cosine algorithm (SCA). The optimization results reveal that the simulation times of the CSA, NNA, GWO, and SCA are 5.2, 6, 5.8, and 5.75 s, respectively. Moreover, the CSA converges to the best minimum within the first 100 iterations, which is faster than the other algorithms. The robustness of the CSA is verified using 20 independent runs, where the CSA achieves the smallest average and standard deviation. In addition, the t-test proves the superiority of the CSA compared to the other algorithms, where all *p*-values are less than 5%. The simulated *I-V* and *I-P* curves of the CSA-PEMFC model match the measured curves very closely. Moreover, the efficacy of the CSA-PEMFC model is evaluated under a variety of temperature and pressure conditions. Therefore, the suggested CSA-PEMFC model has the potential to be an accurate and efficient model.

Keywords: Circle Search Algorithm; fuel cell; optimization; parameters estimation; PEMFC

Citation: Qais, M.H.; Hasanien, H.M.; Turky, R.A.; Alghuwainem, S.; Loo, K.-H.; Elgendy, M. Optimal PEM Fuel Cell Model Using a Novel Circle Search Algorithm. *Electronics* **2022**, *11*, 1808. https://doi.org/10.3390/electronics11121808

Academic Editor: Carlos Andrés García-Vázquez

Received: 27 April 2022
Accepted: 5 June 2022
Published: 7 June 2022

1. Introduction

Fuel cells (FCs) receive considerable interest with regard to producing electricity as alternative energy sources for a variety of reasons, including their high power densities, high power conversion efficiencies, and function as clean energy resources, as well as increased fossil fuel prices [1]. FCs are widely utilized in a variety of industrial applications such as electric vehicles [2], electrical distribution networks, and smart grids [3]. There are numerous fuel cell technologies based on catalytic electrodes and materials [4]. The polymer exchange membrane fuel cell (PEMFC) mixes oxygen and hydrogen without ignition and converts this chemical energy into electrical energy, heat, and water, without pollutant emissions [5]. The PEMFC is the most used technology because of its low working

temperature [6], wide range of pressure, high relative humidity, high power density, fast startup, and low heat waste [7].

Due to the broad application of PEMFCs, their electrical modeling is required by researchers to study their dynamic analysis in industrial and residential applications [8]. A nonlinear model with seven unknown parameters is proposed to find the output voltage of PEMFCs [9,10]. The current-voltage and current-power curves of PEMFCs are utilized in characterizing PEMFCs' performance [11]. Due to the shortage of manufacturers' data, optimization methods are applied to estimate the unknown parameters of the PEMFC model [12]. Usually, optimization methods are utilized to reduce the summation of square errors between estimated voltage and measured voltage data [13]. Optimization constraints include the higher and lower values of the unknown variables.

1.1. Related Work

Several conventional methods were applied to solve the optimization problem and identify the unknown parameters of the fuel cell model. In [14], a simulator with a dynamic model is presented to formulate the optimization problem. The PEMFC dynamic model is introduced in automotive applications [15]. Magnetic field variation in the membrane is emulated using a dipole model, which relies on the superposition concept [16]. Many other conventional methods, such as the stochastic method [13], the input-output diffusive approach [17], and the proper generalized decomposition approach [18] are presented. In this regard, conventional methods suffer from many disadvantages such as (1) they depend on the initial conditions of the problem; (2) they rely on the accuracy of the differential equation solvers [19]; and (3) they may be trapped in a local best solution, not a global solution [20]. It is very difficult for these traditional optimization methods to deal with nonlinear optimization problems such as PEMFC modeling. To avoid this problem, numerous metaheuristic algorithms were used to solve the PEMFC modeling problem.

In the literature review, many metaheuristic algorithms are utilized to find the optimal parameters of the PEMFC model, including the genetic algorithm (GA) [21], particle swarm optimization with neural networks [22], and evolutional and differential evolution algorithms [23,24] including the flower pollination algorithm [25], the harmony search algorithm [26], the neural network algorithm [27], the whale optimization algorithm [28], the Chaos game optimization algorithm [29], and the hunger game search algorithm [30]. Other metaheuristic algorithms are modified to improve their performance for PEMFC modeling, including an improved version of the Archimedes optimization algorithm [31], the chaotic binary shark smell optimization algorithm [32], an extended version of the crow search algorithm [33], hybrid sine cosine and crow search algorithms [34], a Harris hawks optimization algorithm [35], an improved salp swarm algorithm [36], an enhanced transient search optimization algorithm [37,38], and a developed arithmetic optimization algorithm [39]. Although these metaheuristic algorithms are effective [40], some of them suffer from complexity of procedure, long computational time, and immense effort exerted in their design. In today's world, there is a significant revolution of metaheuristic algorithms and artificial intelligence [41].

1.2. Research Gap

The PEMFC model has multiple local optimal solutions that can easily trap optimization algorithms to a local solution. Therefore, most previous research hybridized or modified the applied metaheuristic algorithms to solve this PEMFC model. However, these modifications increase the complexity and execution time of the estimation process. Complex algorithms are not suitable for online parameter estimations of the PEMFC, especially for the control system of the PEMFC stack. Moreover, based on the no-free-launch theorem [42], an invention of a new metaheuristic algorithm or the development of a recent one is highly appreciated. Every new algorithm should provide better results in solving engineering problems; one algorithm may solve one certain problem, but fail to solve a different problem. However, all proposed algorithms were not initially benchmarked using

the fuel cell model. This encouraged the authors to invent a novel optimization algorithm called the Circle Search Algorithm (CSA) and then apply it effortlessly and precisely to the design the PEMFC model.

The CSA is a physics-based metaheuristic algorithm inspired by the geometrical circle [43] which has well known properties, including diameter, center, perimeter, and tangent line. The ratio between the radius and the perpendicular tangent line is the Tan function of the angle opposite to the radius. The Tan function and the opposite angle are utilized in a simple way to model the CSA. The angle of the Tan function plays a crucial role in balancing the exploration and exploitation processes of the CSA. The principal merits of the proposed algorithm include a simple procedure, lower computational burden, and lower design parameters. The CSA will be applied to solve many engineering problems because of its high performance [44].

1.3. Work Contribution

In this paper, a novel CSA is presented with the purpose of obtaining a concise PEMFC model. The proposed algorithm is implemented by minimizing the fitness function, which denotes the summation of square errors between estimated voltage and measured voltage data. The constraints of the optimization problem include the higher and lower values of the design parameters. In this regard, the polarization curves of PEMFCs are utilized in characterizing these fuel cells' performance. These polarization curves are modeled using a nonlinear model, which has seven unknown parameters (ξ_1, ξ_2, ξ_3, ξ_4, λ, R_c and β). ξ_1–ξ_4 are empirical coefficients, λ is a parameter focusing on the relation between water and humidity, R_c represents connection resistance, and β denotes a constant coefficient. Estimation of these unknown parameters is important, as these parameters mainly affect the dynamic analyses of fuel cells in many applications such as electric vehicles and smart grids. Therefore, obtaining a precise model is a vital component of PEMFCs' performance analyses. Different PEMFCs are efficiently modeled, including the Ballard V, BCS-500, and 250 W stack. The simulation results are compared to the measured results. The proposed model is validated by comparing its results to other optimization-based models in the literature. The effectiveness of the proposed model is checked under various temperature and pressure conditions. Its robustness is tested using several statistical analyses involving parametric and nonparametric tests.

The main contributions of this paper can be summarized as follows:

- A novel, efficient, and uncomplicated physics-based metaheuristic algorithm, called the CSA, is presented.
- The proposed CSA is effortlessly employed to identify the unknown parameters of the PEMFC model.
- The CSA optimization results are compared to those attained using the commonly utilized neural network, grey wolf optimization, and sine cosine algorithms.
- The precision of the CSA-PEMFC model is verified by matching the simulated *I-V* and *P-V* curves with the measured curves of three commercial PEMFCs.
- Statistical analyses, including best, average, standard deviation, and *p*-values, are utilized to prove the superiority of the proposed CSA over other algorithms.

This article is structured as follows: Section 2 introduces a nonlinear modeling of the PEM fuel cell and demonstrates the problem formulation. In Section 3, the details and explanation of the CSA are introduced, including its flowchart and mathematical procedures. Section 4 presents and discusses the simulation and experimental results, including robustness analyses. Finally, our conclusion is presented in Section 5.

2. PEMFC Model

The PEMFC mathematical model relies on the well-known Mann model [9], which exhibits the polarization curves of the PEMFC with an efficient and accurate model. It is most commonly used in the literature in modeling this type of fuel cell. In each fuel cell,

there are three voltage quantities; (1) the activation voltage (v_{act}), (2) the ohmic voltage drop (v_{Ω}), and (3) the concentration voltage (v_{con}), as shown in Figure 1 [45].

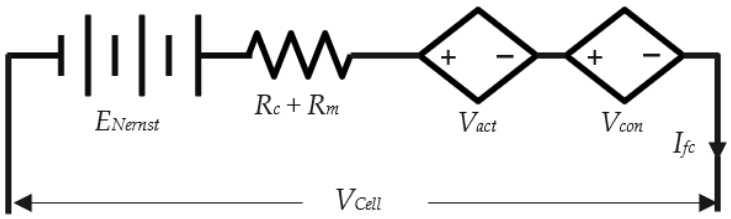

Figure 1. Electrical model of PEMFC.

The PEMFC stack consists of several fuel cells that are connected in series. This stack voltage (V_{Stack}) can be mathematically determined by the following equation:

$$V_{Stack} = N_{cells}.(E_{Nernst} - v_{act} - v_{\Omega} - v_{con}) \tag{1}$$

where N_{cells} represents the total number of fuel cells that are in series connection, and E_{Nernst} denotes the reversible voltage of the fuel cell. The quantity E_{Nernst} can be computed using Equation (2) when room temperature is considered equal to 25 °C. Three voltage drop terms can be mathematically formulated by Equations (3)–(5).

$$E_{Nernst} = 1.229 - 0.85 \times 10^{-3}\left(T_{fc} - 298.15\right) + 4.3085 \times 10^{-5} T_{fc} ln\left(P_{H_2}\sqrt{P_{O_2}}\right) \tag{2}$$

$$\begin{gathered} v_{act} = -\left[\xi_1 + \xi_2 T_{fc} + \xi_3 T_{fc} ln\left(C_{O_2}\right) + \xi_4 T_{fc} ln\left(I_{fc}\right)\right] \\ \text{where } C_{O_2} = \frac{P_{O_2}}{5.08.10^6}.\exp\left(498/T_{fc}\right) \end{gathered} \tag{3}$$

$$\begin{gathered} v_{\Omega} = I_{fc}(R_m + R_c);\ R_m = \frac{\rho_m l}{M_A} \\ \text{where } \rho_m = \frac{181.6\left[1+0.03\left(\frac{I_{fc}}{M_A}\right)+0.062\left(\frac{T_{fc}}{303}\right)^2\left(\frac{I_{fc}}{M_A}\right)^{2.5}\right]}{\left[\lambda-0.634-3\left(\frac{I_{fc}}{M_A}\right)\right]e^{4.18.\frac{T_{fc}-303}{T_{fc}}}} \end{gathered} \tag{4}$$

$$v_{con} = -\beta.ln\left(1 - \frac{J}{J_{max}}\right) \tag{5}$$

where T_{fc} represents the PEMFC temperature (K); P_{H_2} and P_{O_2} represent partial pressures of hydrogen and oxygen (atm), respectively; I_{fc} denotes the fuel cell current (A); M_A is the membrane cross sectional area (cm^2); C_{O_2} represents the oxygen concentration (mol/cm^3); ξ_{1-4} represent semi-empirical factors; R_m denotes a resistance of membrane (Ω); R_c represents a resistance of connections (Ω); l represents the thickness of membrane (cm); ρ_m defines its resistivity $(\Omega.cm)$; λ represents a parameter relating water components to humidity; β represents a constant factor; and J and J_{max} represent the real and maximum values of current density (A/cm^2), respectively.

The prediction of water components is difficult and varies during PEMFC operation. Therefore, the factor λ is equal to 13 at ideal conditions and is 23 at super-saturated conditions. Its maximum value is 23 in this paper. Actually, the value of factor λ is based on the relative humidity and other factors [30].

Notably, the designer needs to optimally estimate seven parameters of the PEMFC model in order to obtain a very concise model. These seven parameters are ξ_1, ξ_2, ξ_3, ξ_4, λ, R_c and β.

The optimization problem of the PEMFC model under study can be mathematically formulated based on the sum of square error criterion; this criterion is the most widely used in the literature. In this regard, the fitness function is defined by the summation of square

errors between the estimated voltage of the model and measured voltage data. The fitness function can be written as follows:

$$fitness = \left(\sum_{i=1}^{N_{samples}} [V_{FC,meas}(i) - V_{FC,est}(i)]^2 \right) \quad (6)$$

where $N_{samples}$ represents the number of measured data; i denotes the counting factor; $V_{FC,meas}$ represents measured output PEMFC voltage (V); and $V_{FC,est}$ is the estimated model voltage (V). The constraints of the optimization problem include the upper and lower values of the seven unknown parameters.

3. Circle Search Algorithm

3.1. Background

The geometrical circle is a basic enclosed arc in which all points are equal in distance from the center. The diameter, as shown in Figure 2, is defined as the line joining two points on the arc that cross at the circle's center (X_c). The radius of the circle is the line that connects any point on it to the center. A circle's perimeter is proportional to the length of the curve that encircles it. A tangential line is a straight line that touches the circle at a single point (X_t) and is orthogonal to the radius that meets this point. According to Pythagorean formulae, the right triangle's orthogonal function (Tan) is the ratio of the radius to the perpendicular tangent line. The radius can be calculated as the distance between X_t and X_c, while the tangent line is defined as the distance between X_t and X_p. Therefore, the orthogonal function (Tan) is defined as in the following equations:

$$\mathrm{Tan}(\theta) = \frac{X_t - X_c}{X_p - X_t} \quad (7)$$

$$X_t - X_c = (X_p - X_t) \times \mathrm{Tan}(\theta) \quad (8)$$

$$X_t = X_c + (X_p - X_t) \times \mathrm{Tan}(\theta) \quad (9)$$

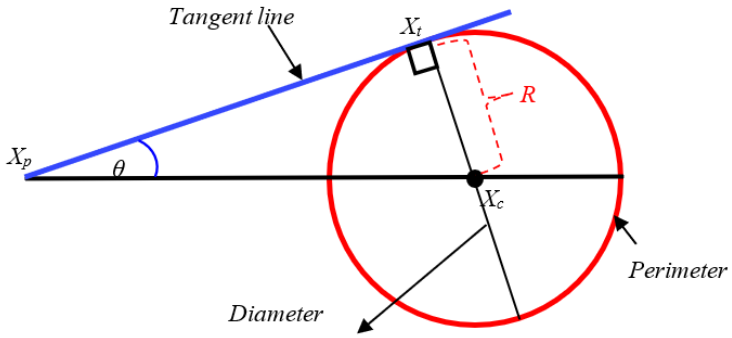

Figure 2. Terms of the geometrical circle.

3.2. CSA Formulation

The CSA searches for the optimal solution within randomized circles in order to broaden the search region. Using the circle's center as a reference point, the angle of the tangential line gradually decreases until it reaches the circle's center, as illustrated in Figure 3a. Due to the probability that this circle was caught in the local solution, the angle of the tangential line varies randomly, as shown in Figure 3b. In the CSA, the touching point X_t is supposed to be the searching agent, and the center point X_c is assumed to be the optimal position. As shown in Figure 3, the CSA updates the search agent in response to the touching point's progress toward the center. To avoid the CSA being trapped in a local

solution, the contact point is changed at random by altering the angle randomly. The steps of the CSA may be described as follows:

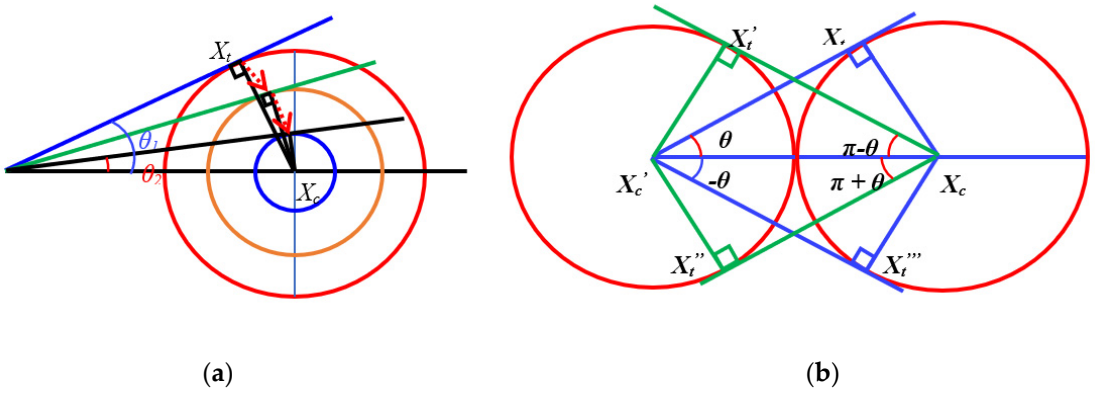

(**a**) (**b**)

Figure 3. The procedures of the CSA: (**a**) exploitation and (**b**) exploration.

Step 1: Initialization: This phase is necessary to the CSA, as it ensures that the entire dimension of each search agent is equally randomized. The majority of previously published code randomly distributes the dimensions, which occasionally gives rise to surprising results from the algorithms. The search agents are initialized among the search space's upper bound (*ub*) and lower bound (*lb*), as specified in Equation (10):

$$X_t = lb + r \times (ub - lb) \tag{10}$$

where r is a real random number between 0 and 1.

Step 2: Varying the agents' locations: The location of the search agent X_t is changed in relation to the assessed best location X_c as shown in Equation (11):

$$X_t = X_c + (X_c - X_t) \times \tan(\theta) \tag{11}$$

where the angle θ shows essential rule in the exploration and exploitation of the CSA and can be calculated as follows:

$$\theta = \begin{cases} a \times rand & r_1 < c \\ a \times \pi & r_1 > c \end{cases} \tag{12}$$

$$a = 2 \times w \times rand - 2 \times w \tag{13}$$

$$w = 1.5 - 1.5 \times \frac{Iter}{Maxiter} \tag{14}$$

where r_1 is a real random number between 0 and 1, *Iter* is the present iteration, *Maxiter* is the total number of iterations, and c is a constant between 0 and 1. Equation (14) shows that the variable w varies from 1.5 to 0 as the iterations number increases. The variable a varies from -3 to 0 based on Equation (13). Consequently, the angle θ varies from $-\frac{3\pi}{2}$ to $\frac{3\pi}{2}$, where $\frac{3}{2} = 1.5$, so it is selected in Equation (14).

There are three states relating to the value of the constant c that can be attained for the CSA as follows:

State 1: c = 0: This leads the angle $\theta = a \times \pi$ all the time, which makes the CSA focus more on the exploitation process.

State 2: c = 1: This leads the angle $\theta = a \times rand$ all the time, which makes the CSA focus more on the exploration process.

State 3: 0 < c < 1: This balances the exploration and exploitation in some optimization problems, where the angle is altered based on the random number r_1. The CSA flowchart is illustrated in Figure 4.

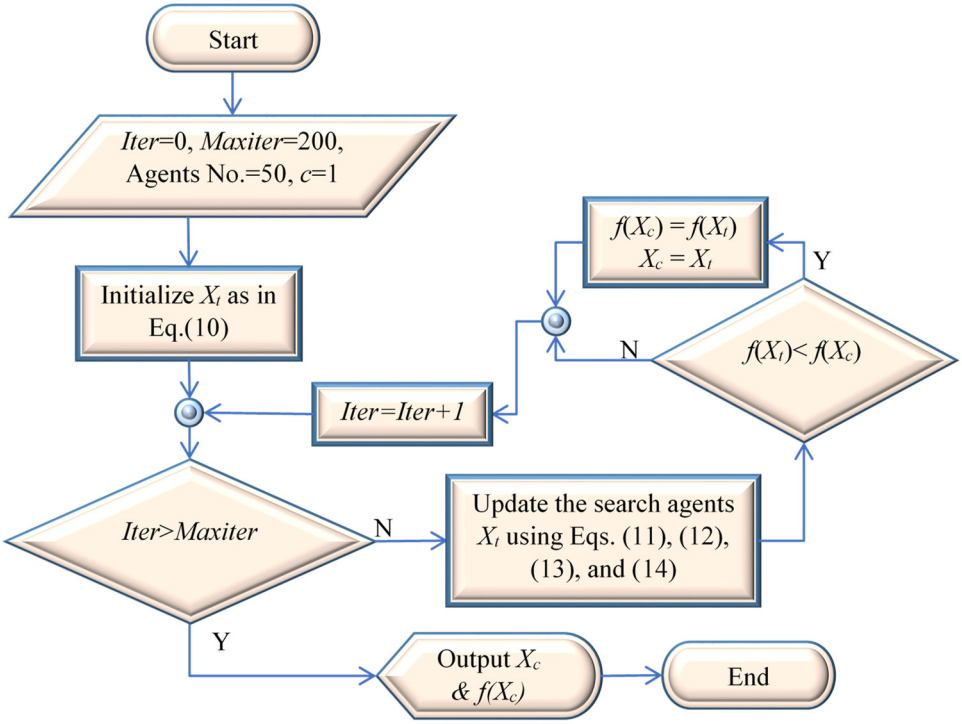

Figure 4. Flowchart of the proposed CSA.

4. Simulation and Experimental Results

In this paper, PEMFC modeling is investigated on three commercial PEMFC stacks. The proposed CSA, the neural network algorithm (NNA), grey wolf optimization (GWO), and the sine cosine algorithm (SCA) are utilized to model these commercial PEMFCs. For a fair comparison, the same initialization, population number of 50, and total iterations of 200 are used for all compared algorithms. These algorithms are utilized to reduce the fitness value that is expressed as the sum of square error between the estimated fuel cell model voltage and the measured voltage. The limits of the estimated parameters are indicated in Table 1. These limits represent the constraints of the optimization problem. The optimization process is carried out using MATLAB software. The simulation results are performed using a Laptop with Intel Core i7-3630, 2.4 GHz, and 8 GB RAM. The following subsections demonstrate the analyses of three PEMFC commercial stacks.

Table 1. Limits of estimated parameters of PEMFC model.

Parameter	ξ_1	ξ_2	ξ_3	ξ_4	λ	$R_c(\mathbf{m\Omega})$	β
Lower	−1.19970	1.000×10^{-3}	3.600×10^{-5}	-26.000×10^{-5}	13.00000	0.10000	0.01360
Upper	−0.85320	5.000×10^{-3}	9.800×10^{-5}	-9.5400×10^{-5}	23.00000	0.80000	0.50000

4.1. Ballard V 5 kW

The Ballard Mark V 5 kW PEMFC stack's information and operating points are recorded in many research papers [46]. This PEMFC possesses 35 cells, which are tied in a series connection. The maximum current is 70 A. The convergence curve of fitness function is illustrated in Figure 5. Notably, in this figure the convergence curve of the proposed CSA is very fast and smoother than that obtained using the other three algorithms. Table 2 lists the optimum parameters of the PEMFC model using the proposed CSA in comparison to other algorithms. It is worth noting that the proposed CSA obtained the best lowest value of the sum of square errors (SSE) when compared to the other algorithms. To examine the superiority of the proposed CSA, 20 independent runs are implemented for all compared al-

gorithms. The statistical results show that the CSA is robust because the average value and standard deviation of SSE for 20 runs are smaller than those of other algorithms, as listed in Table 2. The polarization curves involving *I-V* and *I-P* characteristics are demonstrated in Figure 6a,b, respectively. The simulation results of the estimated PEMFC model parameters using the proposed CSA are very close to the experimental results. This indicates the superiority of the CSA in obtaining a very precise model. Moreover, these polarization curves are investigated under various temperatures and constant partial pressure of oxygen and hydrogen of 1 atm, as shown in Figure 7a,b. Notably, these curves are very smooth without any fluctuations. The PEMFC's voltage and power outputs increase when the temperature increases. Figure 8a,b illustrate polarization curves under various pressures when the temperature is maintained at 70 °C. The voltage and power outputs of the PEMFC increase when the pressure increases. Therefore, the proposed PEMFC model using the CSA can be used to estimate the characteristics of PMEFCs under different operating conditions, such as variation in temperature or partial pressure of oxygen or hydrogen.

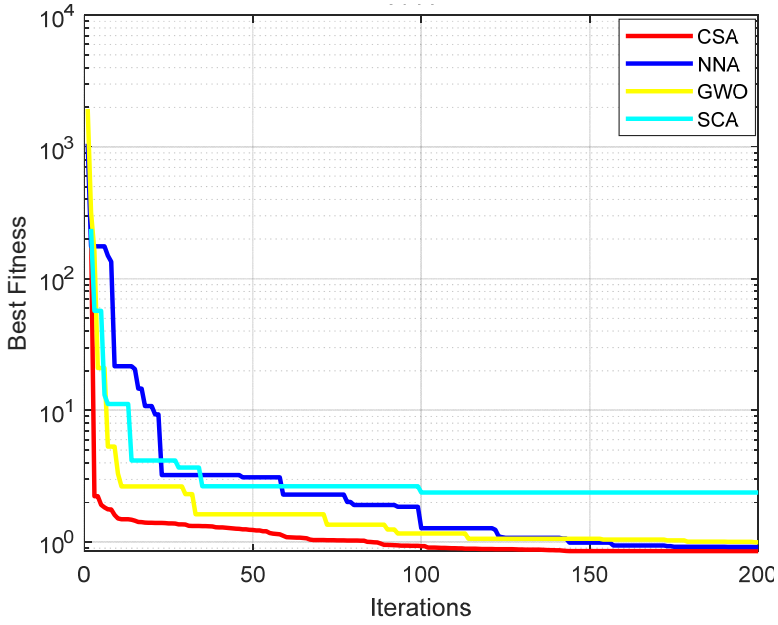

Figure 5. Convergence curve of fitness function for Ballard fuel cell.

Table 2. Optimal parameters of Ballard PEMFC model.

Parameter	CSA	NNA	GWO	SCA
ξ_1	−1.181342405	−1.159421713	−0.904692414	−0.891394545
ξ_2	0.003569096	0.003604278	0.002870928	0.002651533
ξ_3	0.000039929	0.000049260	0.000052237	0.000036000
ξ_4	−0.000162830	−0.000147034	−0.000130626	−0.000156624
λ	23.000000000	23.000000000	23.000000000	23.000000000
R_c	0.000100000	0.000303993	0.000509417	0.000178197
β	0.013600000	0.013601446	0.013643745	0.013600000
Minimum SSE	**0.853607516**	0.87053677	0.857590836	1.097400825
Average SSE	**0.853608540**	0.93009318	0.956658143	1.79161335
Std	**0.000002290**	0.072427297	0.098472885	0.676135903

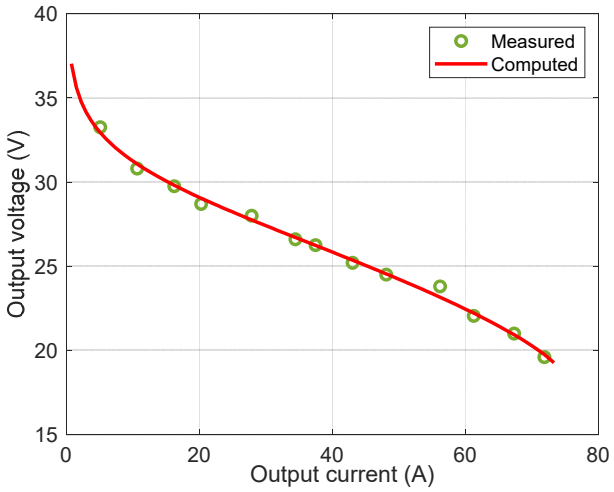

(**a**)

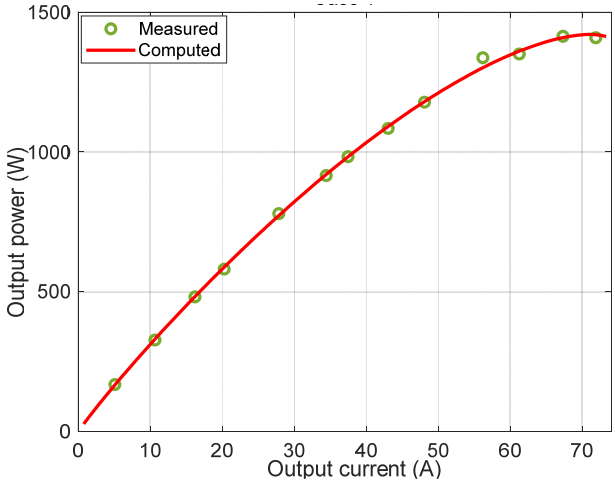

(**b**)

Figure 6. Characteristics of Ballard stack: (**a**) current-voltage and (**b**) current-power.

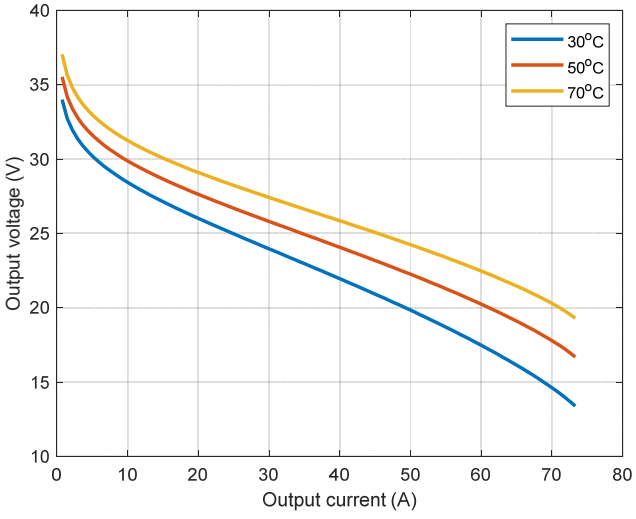

(**a**)

Figure 7. *Cont.*

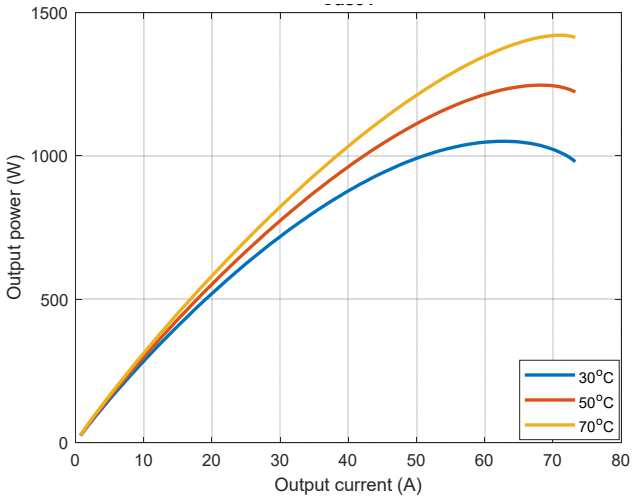

(**b**)

Figure 7. Characteristics of Ballard stack under various temperatures: (**a**) current-voltage and (**b**) current-power.

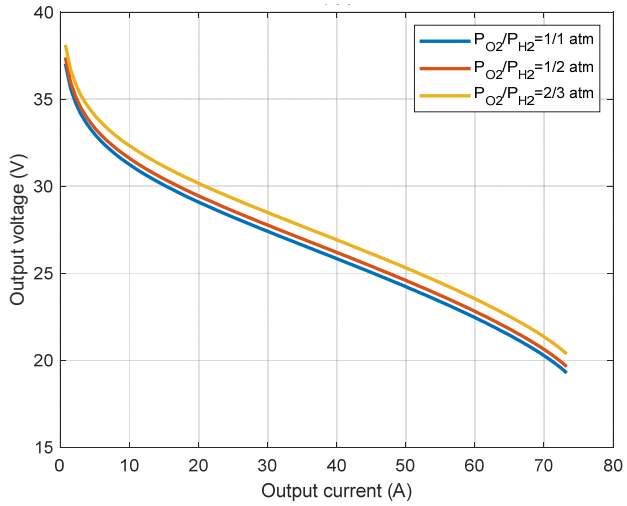

(**a**)

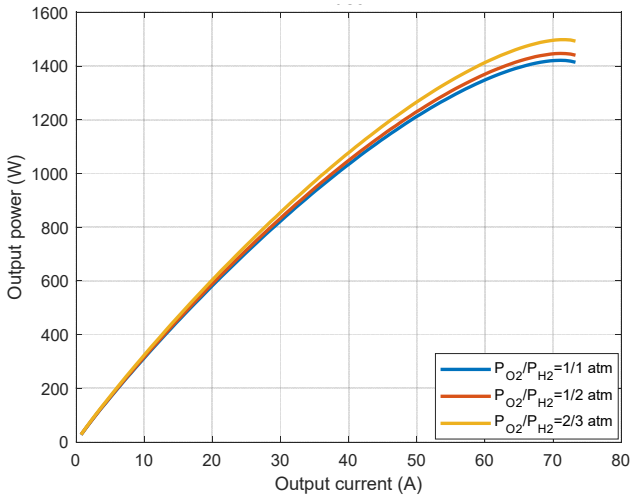

(**b**)

Figure 8. Characteristics of Ballard stack under various pressures: (**a**) current-voltage and (**b**) current-power.

4.2. BCS Fuel Cell

In this subsection, the BCS fuel cell is modeled; its rated power is 500 W. Its data and operating points are described in several research papers [47]. This PEMFC possesses 32 cells, which are tied in a series connection. The maximum current is 30 A. The convergence curves of best values of fitness function with increased iterations for all compared algorithms are illustrated in Figure 9. Notably, this figure shows that the convergence curve of the proposed CSA is very fast, and smoother than that obtained using the NNA, GWO, and SCA algorithms. Table 3 lists the optimum parameters of the PEMFC model using the proposed CSA compared with the other algorithms. The proposed CSA obtained the best minimum of SSE compared with the other algorithms. Moreover, the statistical analysis of the 20 independent runs, including average value and standard deviation, are implemented to test the robustness of the proposed algorithm, which obtained the minimum values among the other algorithms, as listed in Table 3. The polarization curves involving *I-V* and *I-P* characteristics are demonstrated in Figure 10a,b, respectively. The simulation results of the estimated PEMFC model using the proposed CSA are very close to the experimental results. This indicates the outstanding ability of the CSA to obtain a very precise model. These polarization curves are investigated under various temperatures and constant partial pressure of hydrogen and oxygen of 1 atm and 0.2095 atm, respectively, as shown in Figure 11a,b. Notably, these curves are very smooth without any fluctuations. It can be shown that the PEMFC's voltage and power outputs increase when the temperature increases. Figure 12a,b illustrate polarization curves under various pressures when the temperature is maintained at 70 °C. The PEMFC's voltage and power outputs increase when the pressure increases. Therefore, the proposed PEMFC model using the CSA can be used to estimate the characteristics of PEMFCs under different operating conditions, such as variation in temperature or partial pressure of oxygen or hydrogen.

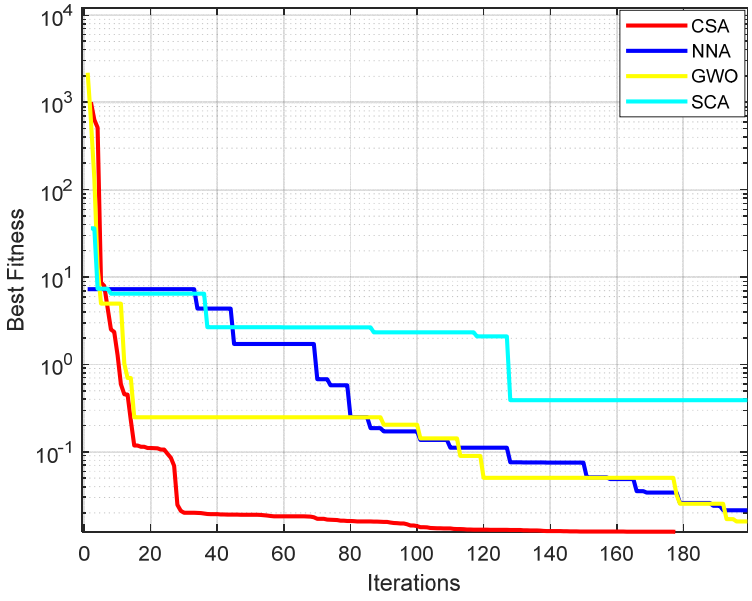

Figure 9. Convergence curve of fitness function for BCS fuel cell.

Table 3. Optimal parameters of BCS PEMFC model.

Parameter	CSA	NNA	GWO	SCA
ξ_1	−1.176591336	−0.872909631	−1.195202326	−0.867565778
ξ_2	0.003496528	0.003189571	0.003627031	0.002527557
ξ_3	0.000058319	0.000097398	0.000063151	0.000053856
ξ_4	−0.000192897	−0.000185976	−0.000191200	−0.000201822
λ	21.324205865	22.996291025	19.262620378	23.000000000

Table 3. *Cont.*

Parameter	CSA	NNA	GWO	SCA
R_c	0.000146406	0.000800000	0.000116867	0.000164497
β	0.016140539	0.013630041	0.014900638	0.018910432
Minimum SSE	**0.011736200**	0.030299900	0.015083800	0.365303000
Average SSE	**0.012154031**	0.103827482	0.020751834	0.637637797
Std	**0.000234547**	0.180842136	0.007801944	0.300158036

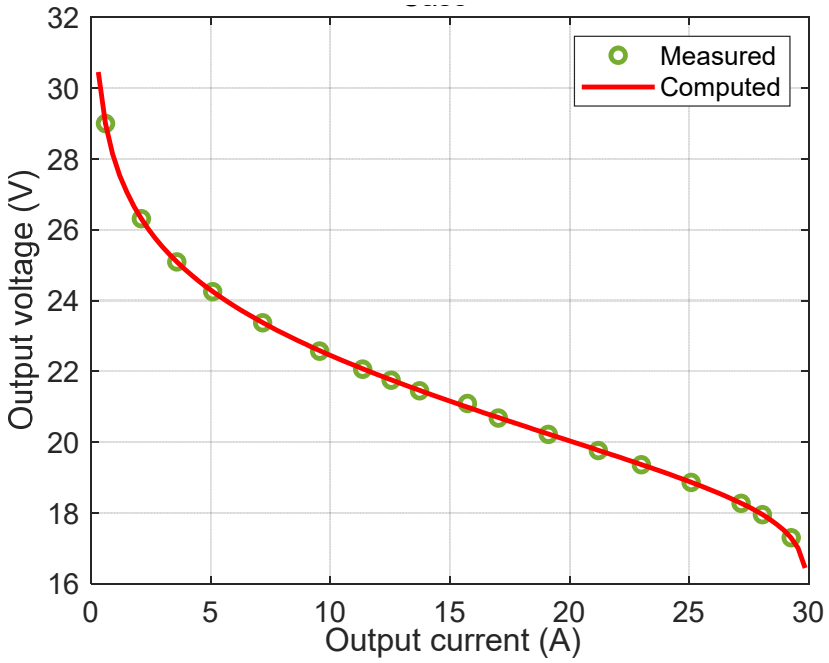

(**a**)

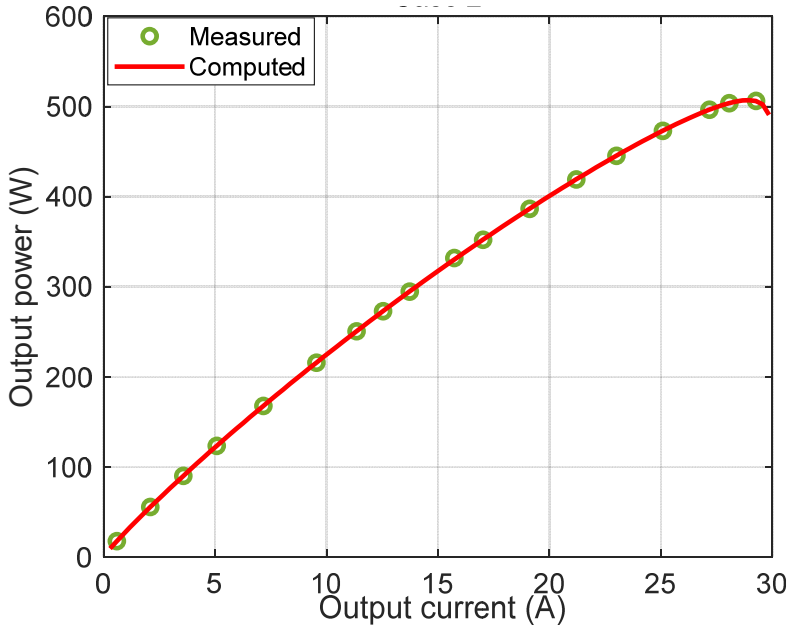

(**b**)

Figure 10. Characteristics of BCS stack: (**a**) current-voltage and (**b**) current-power.

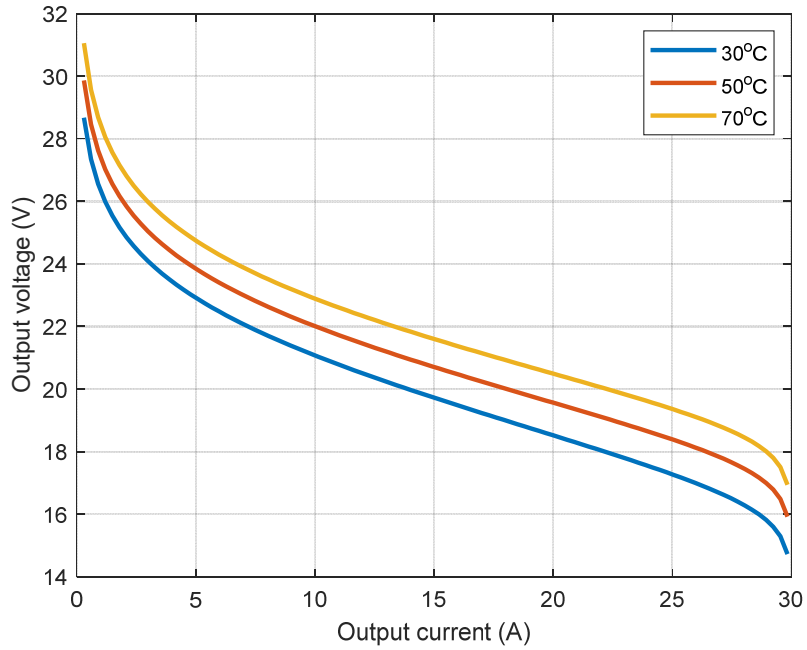

(**a**)

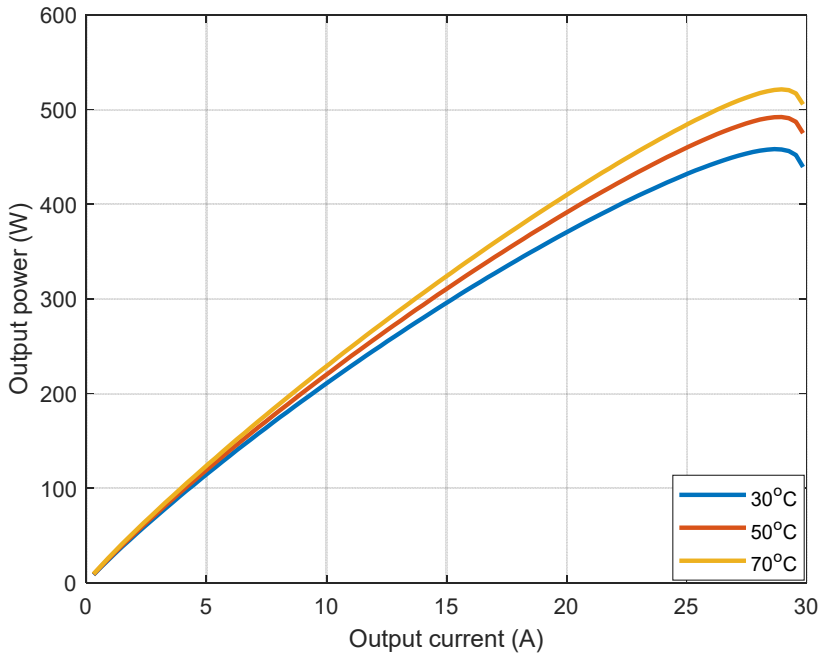

(**b**)

Figure 11. Characteristics of BCS stack under various temperatures: (**a**) current-voltage and (**b**) current-power.

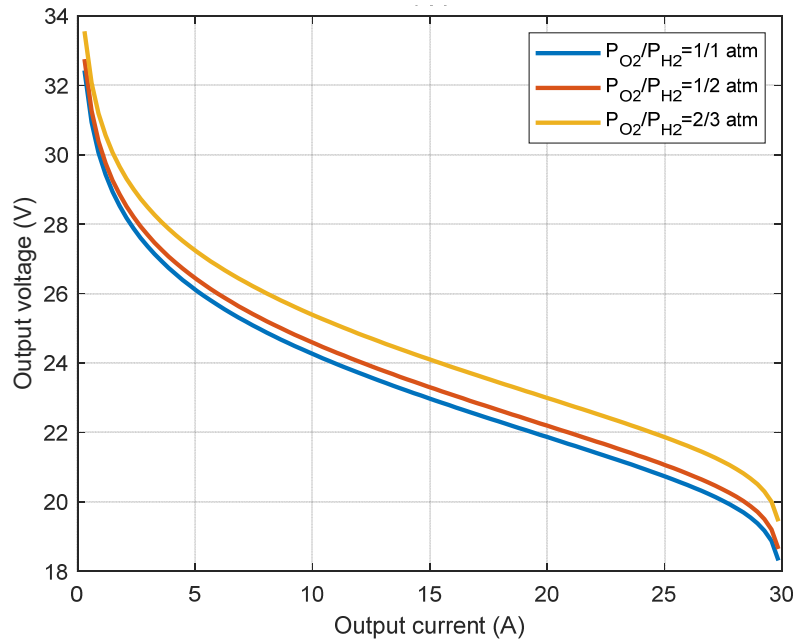

(**a**)

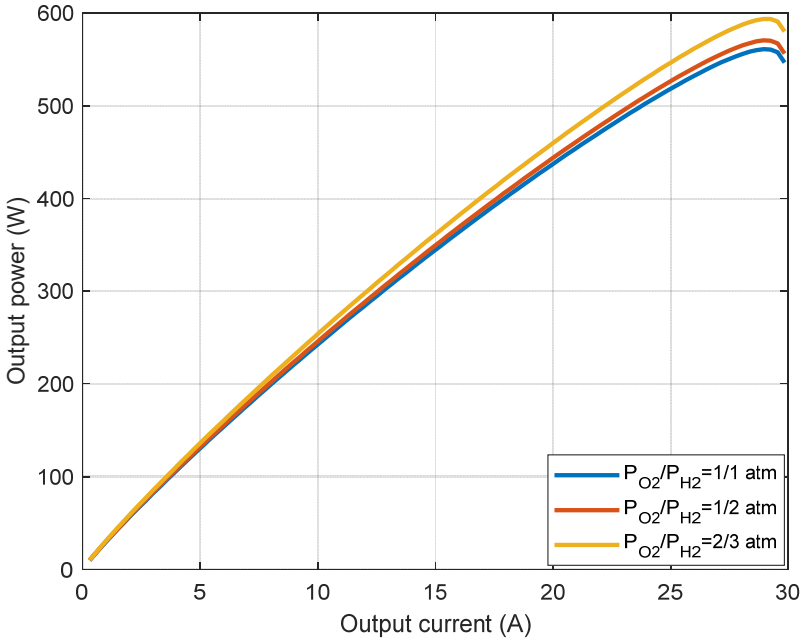

(**b**)

Figure 12. Characteristics of BCS stack under various pressures: (**a**) current-voltage and (**b**) current-power.

4.3. PEMFC 250 W Stack

In this subsection, a PEMFC is modeled; its rated power is 250 W. Its data and operating points are described in several research papers [27]. This PEMFC has 24 cells, which are tied in a series connection. The maximum current density limit due to thermal considerations in this type of PEMFC is 680 mA/cm^2. The convergence curves of best fitness values with increased iterations for all compared algorithms are illustrated in Figure 13. Notably, this figure shows that the convergence curve of the proposed CSA is very fast, and smoother than that obtained using other algorithms such as the NNA, GWO, and SCA. Table 4 lists

the optimum parameters of the PEMFC model using the proposed CSA in comparison with the other algorithms. The proposed CSA obtained the best minimum of the SSE compared to the other algorithms. Moreover, the effectiveness of the proposed CSA is investigated using statistical analysis of the 20 independent runs, where the proposed CSA obtained the minimum average and standard deviation values of all algorithms, as listed in Table 4. The polarization curves involving *I-V* and *I-P* characteristics are demonstrated in Figure 14a,b, respectively. The simulation results of the estimated PEMFC model using the proposed CSA are very close to the experimental results. This indicates the outstanding ability of the CSA to obtain a very precise model. These polarization curves are investigated under various temperatures and constant partial pressure of hydrogen and oxygen of 1 atm, as shown in Figure 15a,b. Notably, these curves are very smooth without any fluctuations. It can be shown that the PEMFC's voltage and power outputs increase when the temperature increases. Figure 16a,b illustrate polarization curves under various pressures when the temperature is maintained at 70 °C. The PEMFC's voltage and power outputs increase when the pressure increases. Therefore, the proposed PEMFC model using the CSA can be used to estimate the characteristics of PEMFCs under different operating conditions such as variation in temperature or partial pressure of oxygen or hydrogen.

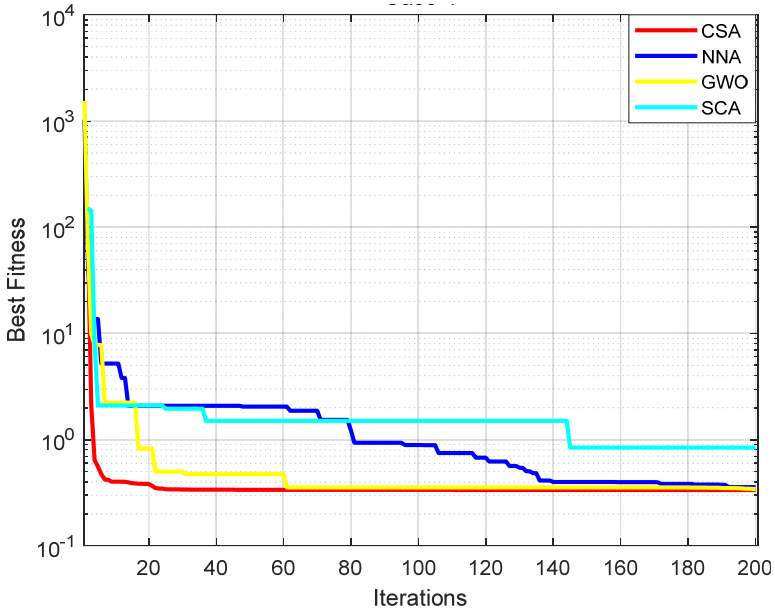

Figure 13. Convergence curve of fitness function for 250 W fuel cell.

Table 4. Optimal parameters of 250 W PEMFC model.

Parameter	CSA	NNA	GWO	SCA
ξ_1	−0.934257737	−1.195665462	−0.853200000	−1.031319464
ξ_2	0.003376648	0.003450698	0.002757282	0.002782153
ξ_3	0.000097994	0.000047760	0.000070814	0.000036000
ξ_4	−0.000174912	−0.000175364	−0.000173435	−0.000156337
λ	19.942856463	22.783534293	21.185483513	18.025697574
R_c	0.000100002	0.000791504	0.000498320	0.000231377
β	0.014534991	0.014495612	0.014599226	0.013600000
Minimum SSE	**0.335980000**	0.342673000	0.338533000	0.425030000
Average SSE	**0.336032627**	0.353771455	0.341326814	0.707907028
Std	**0.000087805**	0.010543026	0.001681107	0.252526872

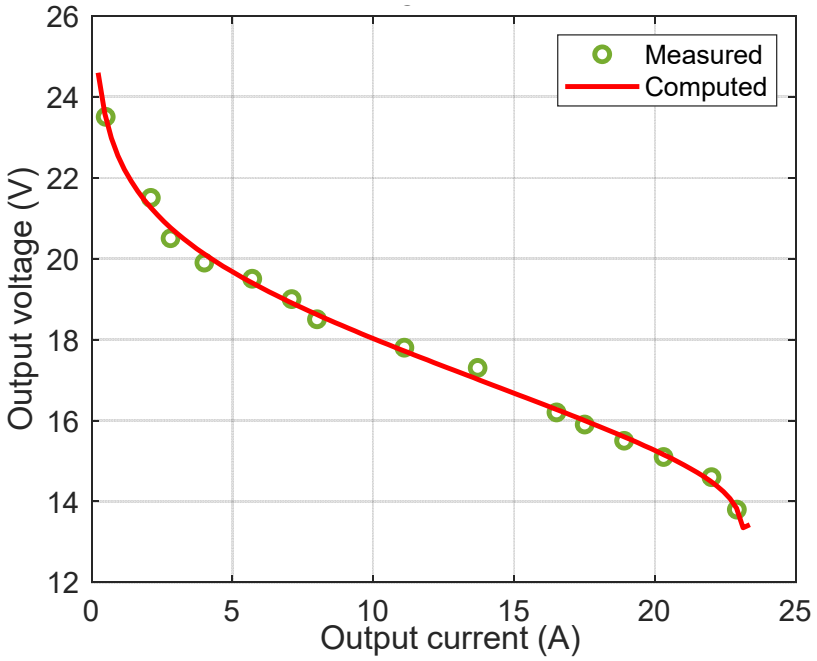

(**a**)

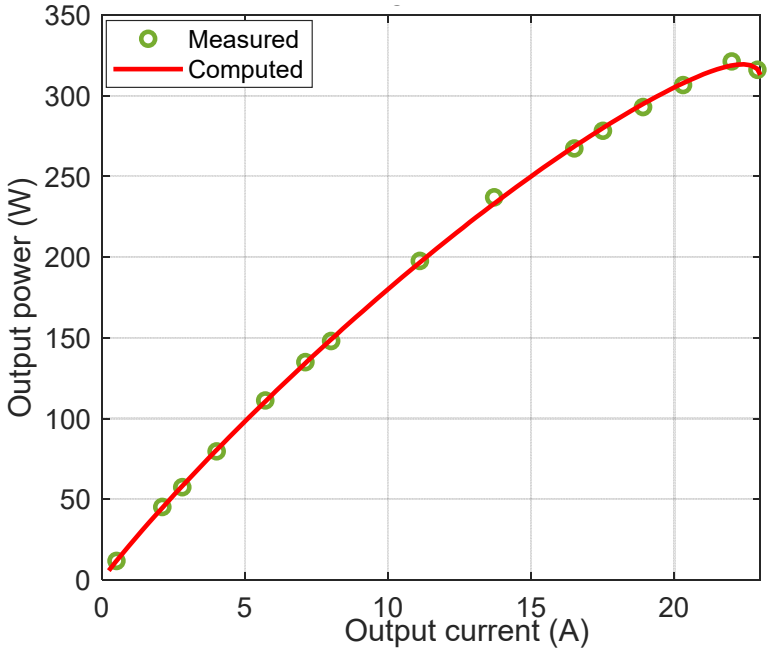

(**b**)

Figure 14. Characteristics of 250 W stack: (**a**) current-voltage and (**b**) current-power.

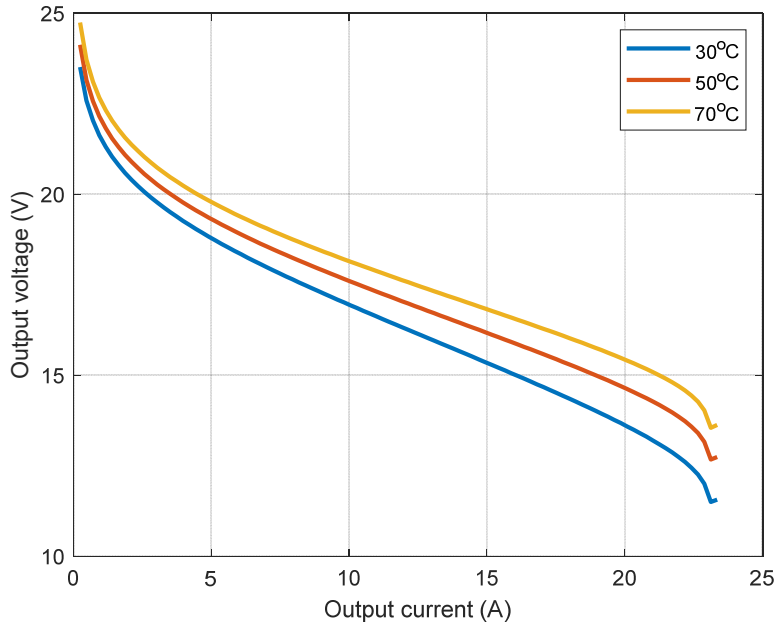

(**a**)

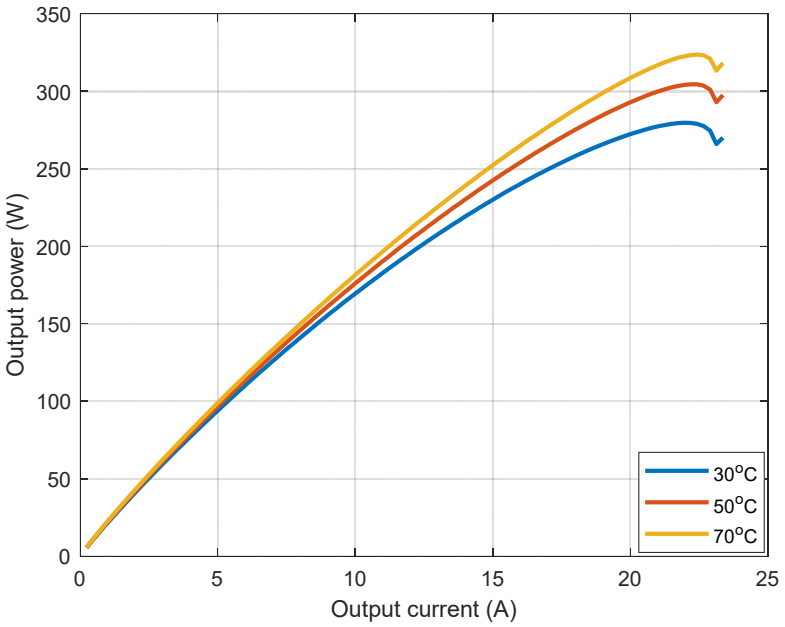

(**b**)

Figure 15. Characteristics of 250 W stack under various temperatures: (**a**) current-voltage and (**b**) current-power.

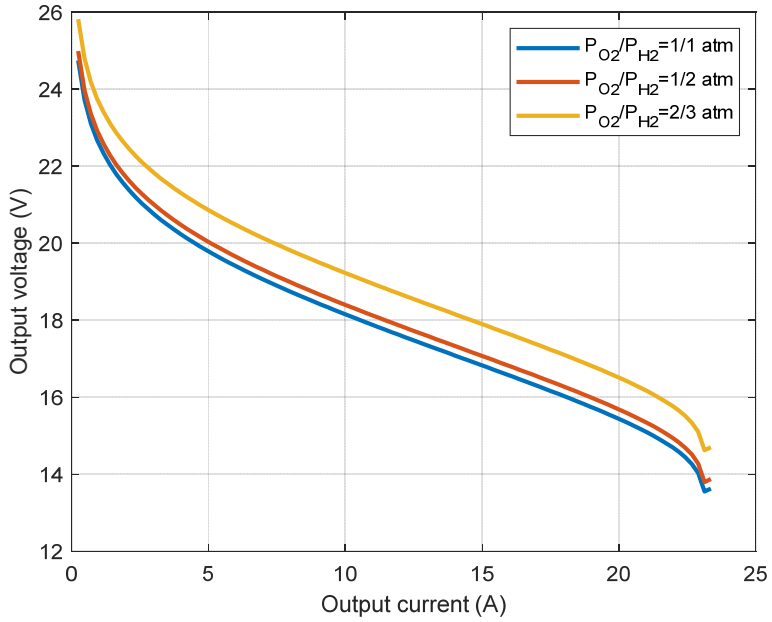

(**a**)

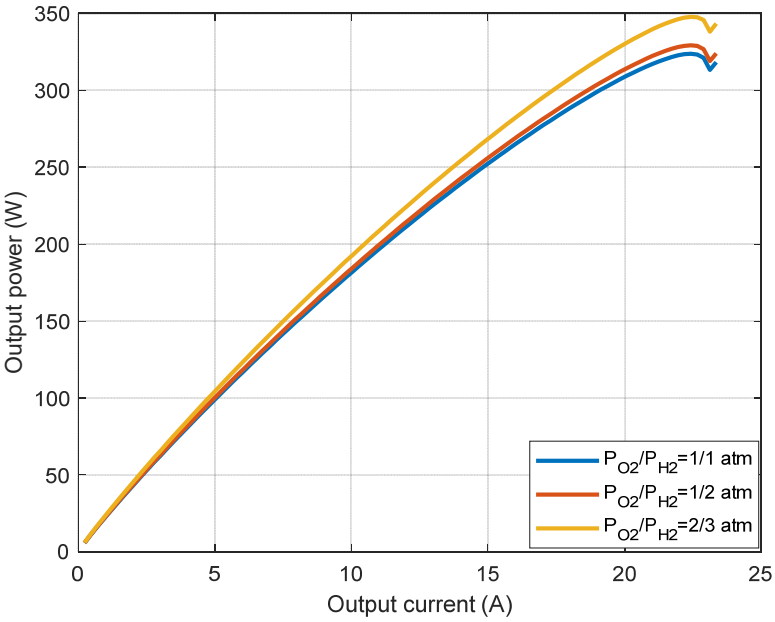

(**b**)

Figure 16. Characteristics of 250 W stack under various pressures: (**a**) current-voltage and (**b**) current-power.

4.4. Superiority Analysis

In this section, the null hypothesis statistical Student's t-test is used to inspect the significance level of the proposed CSA versus other well-known algorithms. In this test, the null hypothesis, which assumes no difference between the results of the proposed CSA and the results of the other algorithms, is rejected if the *p*-value is less than the proposed significance level $\alpha = 5\%$. This t-test is applied to compare the obtained results of 20 independent runs using the CSA, NNA, GWO, and SCA algorithms. Table 5 shows the

p-values of the CSA versus the other algorithms, where all *p*-values are less than 0.05; thus, the significance and superiority of the CSA compared with the other algorithms are proved.

Table 5. The *p*-values of the t-test of the CSA versus other algorithms.

Type	CSA vs. NNA	CSA vs. GWO	CSA vs. SCA
Ballard V 5 kW	0.0037260736	0.0069523914	0.0000623158
BCS Fuel Cell	0.0013970658	0.0136786569	0.0013099501
PEMFC 250 W stack	0.0259578015	0.0086166309	0.0021778679

5. Conclusions

This article proposes a new physics-based metaheuristic algorithm, called the Circle Search Algorithm, which is inspired by the relationship between the radius and perpendicular tangent line of the geometrical circle. The proposed CSA and commonly used NNA, GWO, and SCA are applied to find the anonymous seven parameters of the nonlinear model of the PEMFC. This can be achieved by minimizing the sum of the squared errors (SSEs) between the estimated and measured output voltages of the PEMFC. The optimization algorithms are applied to three commercial PEMFC models by minimizing the SSE value. For an unbiased comparison of the algorithms, they are assigned the same population, initialization, and total number of iterations. The optimization results reveal that the proposed CSA has the fastest simulation time (5.2 s) and convergence speed (within the first 100 iterations) towards the best minimum SSE value compared to the other algorithms. Moreover, the statistical analyses, including average, standard deviation ($<2 \times 10^{-4}$), minimum, and *p*-values (<0.05), verify the superiority of the proposed CSA versus the other algorithms. The estimated *I-V* and *I-P* curves of the CSA-PEMFC are compared with the measured curves illustrating the precision of the proposed CSA-PEMFC model. The proposed CSA-PEMFC model is examined at different temperatures and pressures. In conclusion, the proposed CSA is an efficient algorithm that can be applied to different engineering problems. Therefore, it will be utilized to solve other optimization problems in the future, including those associated with renewable energy, power systems, and smart grid applications.

Author Contributions: Conceptualization, M.H.Q.; data curation, S.A.; formal analysis, M.H.Q., H.M.H., R.A.T., S.A., K.-H.L. and M.E.; investigation, H.M.H., R.A.T. and K.-H.L.; methodology, M.H.Q.; project administration, S.A.; resources, M.E.; software, M.H.Q.; supervision, S.A. and K.-H.L.; visualization, H.M.H., R.A.T. and M.E.; writing—original draft, M.H.Q.; writing—review and editing, H.M.H., M.E. and K.-H.L. All authors have read and agreed to the published version of the manuscript.

Funding: This work was supported by the Researchers Supporting Project number (RSP-2021/307), King Saud University, Riyadh, Saudi Arabia.

Institutional Review Board Statement: Not applicable.

Informed Consent Statement: Not applicable.

Data Availability Statement: Not applicable.

Acknowledgments: This work was supported by the Researchers Supporting Project number (RSP-2021/307), King Saud University, Riyadh, Saudi Arabia.

Conflicts of Interest: The authors declare no conflict of interest.

References

1. Xiong, K.; Wu, W.; Wang, S.; Zhang, L. Modeling, design, materials and fabrication of bipolar plates for proton exchange membrane fuel cell: A review. *Appl. Energy* **2021**, *301*, 117443. [CrossRef]
2. Al-Hamed, K.; Dincer, I. A novel ammonia molten alkaline fuel cell based integrated powering system for clean rail transportation. *Energy* **2020**, *201*, 117620. [CrossRef]

3. Oldenbroek, V.; Wijtzes, S.; Blok, K.; van Wijk, A.J. Fuel cell electric vehicles and hydrogen balancing 100 percent renewable and integrated national transportation and energy systems. *Energy Convers. Manag. X* **2021**, *9*, 100077. [CrossRef]
4. Zhang, X.; Zhang, T.; Chen, H.; Cao, Y. A review of online electrochemical diagnostic methods of on-board proton exchange membrane fuel cells. *Appl. Energy* **2021**, *286*, 116481. [CrossRef]
5. Wang, Y.; Diaz, D.F.R.; Chen, K.S.; Wang, Z.; Adroher, X.C. Materials, technological status, and fundamentals of PEM fuel cells—A review. *Mater. Today* **2020**, *32*, 178–203. [CrossRef]
6. Song, Z.; Pan, Y.; Chen, H.; Zhang, T. Effects of temperature on the performance of fuel cell hybrid electric vehicles: A review. *Appl. Energy* **2021**, *302*, 117572. [CrossRef]
7. Sharaf, O.Z.; Orhan, M.F. An overview of fuel cell technology: Fundamentals and applications. *Renew. Sustain. Energy Rev.* **2014**, *32*, 810–853. [CrossRef]
8. Uzunoglu, M.; Alam, M. Dynamic modeling, design, and simulation of a combined PEM fuel cell and ultracapacitor system for stand-alone residential applications. *IEEE Trans. Energy Convers.* **2006**, *21*, 767–775. [CrossRef]
9. Mann, R.F.; Amphlett, J.C.; Hooper, M.A.I.; Jensen, H.M.; Peppley, B.A.; Roberge, P.R. Development and application of a generalised steady-state electrochemical model for a PEM fuel cell. *J. Power Sources* **2000**, *86*, 173–180. [CrossRef]
10. Correa, J.; Farret, F.A.; Canha, L.; Simoes, M. An Electrochemical-based fuel-cell model suitable for electrical engineering automation approach. *IEEE Trans. Ind. Electron.* **2004**, *51*, 1103–1112. [CrossRef]
11. Chen, M.; Rincon-Mora, G. A Compact electrical model for microscale fuel cells capable of predicting runtime and I–V polarization performance. *IEEE Trans. Energy Convers.* **2008**, *23*, 842–850. [CrossRef]
12. Omran, A.; Lucchesi, A.; Smith, D.; Alaswad, A.; Amiri, A.; Wilberforce, T.; Sodré, J.R.; Olabi, A. Mathematical model of a proton-exchange membrane (PEM) fuel cell. *Int. J. Thermofluids* **2021**, *11*, 100110. [CrossRef]
13. Alotto, P.; Guarnieri, M. Stochastic methods for parameter estimation of multiphysics models of fuel cells. *IEEE Trans. Magn.* **2014**, *50*, 701–704. [CrossRef]
14. Voottipruex, K.; Sangswang, A.; Naetiladdanon, S.; Mujjalinvimut, E.; Wongyoa, N. PEM fuel cell emulator based on dynamic model with relative humidity calculation. In Proceedings of the 14th International Conference on Electrical Engineering/Electronics, Computer, Telecommunications and Information Technology (ECTI-CON), Phuket, Thailand, 27–30 June 2017; pp. 529–532. [CrossRef]
15. Rabbani, R.A.; Rokni, M. Dynamic simulation of a proton exchange membrane fuel cell system for automotive applications. In Proceedings of the Proceedings of SEEP2012, Dublin, Ireland, 5–8 June 2012; pp. 311–316.
16. Claycomb, J.R. Algorithms for the magnetic assessment of Proton Exchange Membrane (PEM) fuel cells. *Res. Nondestruct. Eval.* **2017**, *29*, 167–182. [CrossRef]
17. Restrepo, C.; Garcia, G.; Calvente, J.; Giral, R.; Martinez-Salamero, L. Static and dynamic current–voltage modeling of a proton exchange membrane fuel cell using an input–output diffusive approach. *IEEE Trans. Ind. Electron.* **2015**, *63*, 1003–1015. [CrossRef]
18. Alotto, P.; Guarnieri, M.; Moro, F.; Stella, A. A proper generalized decomposition approach for fuel cell polymeric membrane modeling. *IEEE Trans. Magn.* **2011**, *47*, 1462–1465. [CrossRef]
19. Qais, M.; Hasanien, H.M.; Alghuwainem, S. Output power smoothing of grid-connected permanent-magnet synchronous generator driven directly by variable speed wind turbine: A review. *J. Eng.* **2017**, *2017*, 1755–1759. [CrossRef]
20. Niu, Q.; Zhang, L.; Li, K. A biogeography-based optimization algorithm with mutation strategies for model parameter estimation of solar and fuel cells. *Energy Convers. Manag.* **2014**, *86*, 1173–1185. [CrossRef]
21. Li, W.-Z.; Yang, W.-W.; Wang, N.; Jiao, Y.-H.; Yang, Y.; Qu, Z.-G. Optimization of blocked channel design for a proton exchange membrane fuel cell by coupled genetic algorithm and three-dimensional CFD modeling. *Int. J. Hydrogen Energy* **2020**, *45*, 17759–17770. [CrossRef]
22. Chen, K.; Laghrouche, S.; Djerdir, A. Degradation prediction of proton exchange membrane fuel cell based on grey neural network model and particle swarm optimization. *Energy Convers. Manag.* **2019**, *195*, 810–818. [CrossRef]
23. Restrepo, C.; Konjedic, T.; Garces, A.; Calvente, J.; Giral, R. Identification of a proton-exchange membrane fuel cell's model parameters by means of an evolution strategy. *IEEE Trans. Ind. Inform.* **2014**, *11*, 548–559. [CrossRef]
24. Sun, Z.; Cao, D.; Ling, Y.; Xiang, F.; Sun, Z.; Wu, F. Proton exchange membrane fuel cell model parameter identification based on dynamic differential evolution with collective guidance factor algorithm. *Energy* **2020**, *216*, 119056. [CrossRef]
25. Priya, K.; Rajasekar, N. Application of flower pollination algorithm for enhanced proton exchange membrane fuel cell modelling. *Int. J. Hydrogen Energy* **2019**, *44*, 18438–18449. [CrossRef]
26. Askarzadeh, A.; Rezazadeh, A. A grouping-based global harmony search algorithm for modeling of proton exchange membrane fuel cell. *Int. J. Hydrogen Energy* **2011**, *36*, 5047–5053. [CrossRef]
27. Fawzi, M.; El-Fergany, A.A.; Hasanien, H.M. Effective methodology based on neural network optimizer for extracting model parameters of PEM fuel cells. *Int. J. Energy Res.* **2019**, *43*, 8136–8147. [CrossRef]
28. El-Fergany, A.A.; Hasanien, H.M.; Agwa, A.M. Semi-empirical PEM fuel cells model using whale optimization algorithm. *Energy Convers. Manag.* **2019**, *201*, 112197. [CrossRef]
29. Alsaidan, I.; Shaheen, M.; Hasanien, H.; Alaraj, M.; Alnafisah, A. Proton exchange membrane fuel cells modeling using chaos game optimization technique. *Sustainability* **2021**, *13*, 7911. [CrossRef]

30. Fahim, S.R.; Hasanien, H.M.; Turky, R.A.; Alkuhayli, A.; Al-Shamma'A, A.A.; Noman, A.M.; Tostado-Véliz, M.; Jurado, F. Parameter identification of proton exchange membrane fuel cell based on hunger games search algorithm. *Energies* **2021**, *14*, 5022. [CrossRef]
31. Yao, B.; Hayati, H. Model parameters estimation of a proton exchange membrane fuel cell using improved version of Archimedes optimization algorithm. *Energy Rep.* **2021**, *7*, 5700–5709. [CrossRef]
32. Wei, Y.; Stanford, R.J. Parameter identification of solid oxide fuel cell by chaotic binary shark smell optimization method. *Energy* **2019**, *188*, 115770. [CrossRef]
33. Lu, X.; Kanghong, D.; Guo, L.; Wang, P.; Yildizbasi, A. Optimal estimation of the proton exchange membrane fuel cell model parameters based on extended version of crow search algorithm. *J. Clean. Prod.* **2020**, *272*, 122640. [CrossRef]
34. Alizadeh, M.; Torabi, F. Precise PEM fuel cell parameter extraction based on a self-consistent model and SCCSA optimization algorithm. *Energy Convers. Manag.* **2020**, *229*, 113777. [CrossRef]
35. Yousri, D.; Mirjalili, S.; Machado, J.T.; Thanikanti, S.B.; Elbaksawi, O.; Fathy, A. Efficient fractional-order modified Harris hawks optimizer for proton exchange membrane fuel cell modeling. *Eng. Appl. Artif. Intell.* **2021**, *100*, 104193. [CrossRef]
36. Sultan, H.M.; Menesy, A.S.; Kamel, S.; Selim, A.; Jurado, F. Parameter identification of proton exchange membrane fuel cells using an improved salp swarm algorithm. *Energy Convers. Manag.* **2020**, *224*, 113341. [CrossRef]
37. Hasanien, H.M.; Shaheen, M.A.; Turky, R.A.; Qais, M.H.; Alghuwainem, S.; Kamel, S.; Tostado-Véliz, M.; Jurado, F. Precise modeling of PEM fuel cell using a novel enhanced transient search optimization algorithm. *Energy* **2022**, *247*, 123530. [CrossRef]
38. Qais, M.H.; Hasanien, H.M.; Alghuwainem, S. Optimal transient search algorithm-based PI controllers for enhancing low voltage ride-through ability of grid-linked PMSG-based wind turbine. *Electronics* **2020**, *9*, 1807. [CrossRef]
39. Xu, Y.-P.; Tan, J.-W.; Zhu, D.-J.; Ouyang, P.; Taheri, B. Model identification of the proton exchange membrane fuel cells by extreme learning machine and a developed version of arithmetic optimization algorithm. *Energy Rep.* **2021**, *7*, 2332–2342. [CrossRef]
40. Qais, M.H.; Hasanien, H.M.; Alghuwainem, S.; Elgendy, M.A. Output power smoothing of grid-tied PMSG-based variable speed wind turbine using optimal controlled SMES. In Proceedings of the 54th International Universities Power Engineering Conference (UPEC), Bucharest, Romania, 3–6 September 2019; pp. 1–6. [CrossRef]
41. Qais, M.; AbdulWahid, Z. A new method for improving particle swarm optimization algorithm (TriPSO). In Proceedings of the 2013 5th International Conference on Modeling, Simulation and Applied Optimization (ICMSAO), Hammamet, Tunisia, 28–30 April 2013.
42. Wolpert, D.H.; Macready, W.G. No free lunch theorems for optimization. *IEEE Trans. Evol. Comput.* **1997**, *1*, 67–82. [CrossRef]
43. Qais, M.H.; Hasanien, H.M.; Turky, R.A.; Alghuwainem, S.; Tostado-Véliz, M.; Jurado, F. Circle Search Algorithm: A Geometry-Based Metaheuristic Optimization Algorithm. *Mathematics* **2022**, *10*, 1626. [CrossRef]
44. Qais, M.H.; Hasanien, H.M.; Alghuwainem, S.; Loo, K.; Elgendy, M.; Turky, R.A. Accurate three-diode model estimation of photovoltaic modules using a novel circle search algorithm. *Ain Shams Eng. J.* **2022**, 101824. [CrossRef]
45. Atlam, Ö.; Dündar, G. A practical equivalent electrical circuit model for proton exchange membrane fuel cell (PEMFC) systems. *Int. J. Hydrogen Energy* **2021**, *46*, 13230–13239. [CrossRef]
46. El-Fergany, A.A. Electrical characterisation of proton exchange membrane fuel cells stack using grasshopper optimiser. *IET Renew. Power Gener.* **2018**, *12*, 9–17. [CrossRef]
47. Rao, Y.; Shao, Z.; Ahangarnejad, A.H.; Gholamalizadeh, E.; Sobhani, B. Shark smell optimizer applied to identify the optimal parameters of the proton exchange membrane fuel cell model. *Energy Convers. Manag.* **2019**, *182*, 1–8. [CrossRef]